Developmental Cell, Vol. 6, 511–523, April, 2004, Copyright ©2004 by Cell Press

Centrosome Maturation and Duplication in *C. elegans* Require the Coiled-Coil Protein SPD-2

Catherine A. Kemp,[1] Kevin R. Kopish,[2] Peder Zipperlen,[3] Julie Ahringer,[3] and Kevin F. O'Connell[1,*]
[1]Laboratory of Biochemistry and Genetics
National Institute of Diabetes and Digestive and Kidney Diseases
National Institutes of Health
Bethesda, Maryland 20892
[2]Promega Corporation
2800 Woods Hollow Road
Madison, Wisconsin 53711
[3]Wellcome Trust/Cancer Research UK Institute
University of Cambridge
Tennis Court Road
CB2 1QR Cambridge
United Kingdom

Summary

Centrosomes are major determinants of mitotic spindle structure, but the mechanisms regulating their behavior remain poorly understood. The *spd-2* gene of *C. elegans* is required for centrosome assembly or "maturation." Here we show that *spd-2* encodes a coiled-coil protein that localizes within pericentriolar material (PCM) and in the immediate vicinity of centrioles. During maturation, SPD-2 gradually accumulates at the centrosome in a manner that is partially dependent on Aurora-A kinase and cytoplasmic dynein. Interestingly, SPD-2 interacts genetically with dynein heavy chain and SPD-5, another coiled-coil protein required for centrosome maturation. SPD-2 and SPD-5 are codependent for localization to the PCM, but SPD-2 localizes to centrioles independently of SPD-5. Surprisingly, we also find that SPD-2 is required for centrosome duplication and genetically interacts with ZYG-1, a kinase required for duplication. Thus, we have identified SPD-2 as a factor critical for the two basic functions of the centrosome—microtubule organization and duplication.

Introduction

The centrosome is the primary microtubule-organizing center (MTOC) of the cell and in metazoans consists of a pair of centrioles surrounded by a matrix of microtubule-nucleating pericentriolar material (PCM) (for review see Balczon, 1996; Bornens, 2002; Tassin and Bornens, 1999). Centrosomes order the interphase cytoplasm and play a major role in establishing the structure of the mitotic spindle. To accomplish these tasks, the replication and microtubule-nucleating capacity of the centrosome must be precisely regulated during the cell cycle (Palazzo et al., 2000; Sluder and Hinchcliffe, 1999). Duplication of the centrosome initiates around the time of S phase and completes before mitosis so that two centrosomes are available to form the poles of the bipolar spindle. Duplication involves the splitting of a centriole pair followed by the synthesis of a new centriole adjacent to each preexisting centriole (Kuriyama and Borisy, 1981). The replicated centrosomes then migrate apart in preparation for spindle assembly. As cells progress toward mitosis, the size and microtubule-nucleating capacity of the centrosome increase, a process termed maturation (reviewed in Palazzo et al., 2000). Maturation involves the recruitment of PCM components such as γ-tubulin (Stearns and Kirschner, 1994) and pericentrin (Doxsey et al., 1994) from cytoplasmic stores and has been intensively studied in embryonic systems, in which an initially inactive sperm-derived centriole pair must accrue PCM components from the oocyte cytoplasm to become a full-fledged MTOC.

To date, a number of important regulatory factors that govern maturation and duplication have been identified, but there exists only fragmentary knowledge of how these processes work on a molecular level. Maturation is known to involve the activities of several serine/threonine kinase families. Among these, Polo-like kinases have emerged as key regulators of centrosome function (Dai et al., 2002; Donaldson et al., 2001a). In *Drosophila*, Polo is required for recruitment of γ-tubulin and the protein CP190 to centrosomes (Donaldson et al., 2001b) and in vitro phosphorylates Asp, a microtubule-associated protein required for normal spindle morphology (do Carmo Avides et al., 2001). Centrosome maturation is also regulated by members of the Aurora-A kinase family (Blagden and Glover, 2003; Katayama et al., 2003). In *Drosophila*, Aurora-A is required for association of γ-tubulin and Centrosomin with the centrosome of mitotic cells (Berdnik and Knoblich, 2002), and, in *C. elegans*, Aurora-A is required for a microtubule-independent increase in PCM components (Hannak et al., 2001).

A hierarchy of kinases also regulates duplication of the centrosome. Initiation of centrosome duplication is regulated by the kinase cdk2-cyclin E/A (Hinchcliffe et al., 1999; Lacey et al., 1999; Matsumoto et al., 1999; Meraldi et al., 1999), and three targets of this kinase, nucleophosmin (Okuda et al., 2000), the kinase MPS1 (Fisk and Winey, 2001), and CP110 (Chen et al., 2002) have been implicated in the early phases of duplication. Additional studies have identified factors that regulate later steps in the pathway. Assembly of new centrioles—which contain a 9-fold symmetric arrangement of singlet, doublet, or triplet microtubules—has been shown to require centrin-2 in mammals (Salisbury et al., 2002) and the kinase ZYG-1 (O'Connell et al., 2001) and the coiled-coil protein SAS-4 (Kirkham et al., 2003; Leidel and Gonczy, 2003) in *C. elegans*. Interestingly, γ-tubulin has also been implicated in this step in *Paramecium* and *Tetrahymena* (Ruiz et al., 1999; Shang et al., 2002) and presumably acts to nucleate assembly of the microtubules that constitute the centriole walls. This exciting finding suggests that the processes of duplication and maturation might utilize a number of common factors.

The *C. elegans* embryo has emerged as a powerful

*Correspondence:: kevino@intra.niddk.nih.gov

model system for the identification and analysis of factors regulating diverse aspects of cell division (for review see Bowerman, 2001; Gonczy, 2002; O'Connell, 2000). In addition to Aurora-A, centrosome maturation in the *C. elegans* embryo requires SPD-5, a coiled-coil domain-containing PCM component (Hamill et al., 2002), and *spd-2*, an essential gene of unknown molecular identity (O'Connell et al., 2000). Here we report the cloning and analysis of the *spd-2* gene and reveal that SPD-2, like SPD-5 and many other centrosome components, contains regions predicted to form coiled coils. We find that SPD-2 localizes to both centrioles and PCM and that it acts early in the morphogenetic pathway of PCM assembly. We show that SPD-2 localization involves the activities of a subset of centrosome-associated factors and that in addition to its role in maturation, SPD-2 is required for duplication and interacts genetically with components of both the maturation and duplication pathways.

Results

SPD-2 Encodes a Protein with Three Coiled-Coil Domains

Centrosome maturation and spindle assembly in the *C. elegans* embryo require the *spd-2* gene (O'Connell et al., 2000). In embryos with reduced *spd-2* activity, centrosomes recruit only trace amounts of γ-tubulin and nucleate only a small number of astral microtubules. As a result, bipolar spindles fail to assemble. All known alleles of this gene are recessive loss-of-function mutations and produce a strict maternal-effect temperature-sensitive (ts) embryonic lethal phenotype (O'Connell et al., 1998, 2000). The strongest alleles also exhibit a number of postembryonic defects, indicating that *spd-2* functions throughout development (O'Connell et al., 1998). The embryonic phenotypes described in this paper are not modified by fertilization with wild-type sperm (unpublished data), and are thus solely due to the absence of maternally expressed SPD-2 protein.

To investigate the function of *spd-2* at a molecular level, we identified the corresponding open reading frame. Previously, we mapped the *spd-2* gene to position 3.27 map units on linkage group I (O'Connell et al., 1998). A survey of genes in the region revealed that one, F32H2.3, possessed an RNAi phenotype essentially identical to that of *spd-2* mutants (Figure 1 and Kamath et al., 2001). Specifically, both mutant and RNAi-treated embryos lacked a pseudocleavage furrow, exhibited defects in pronuclear migration, and failed to assemble a bipolar spindle and divide (Compare Figure 1A to 1B and 1C). We also used RNAi to block expression of the F32H2.3 gene in a strain expressing GFP-α-tubulin. Loss of F32H2.3 expression led to a profound defect in microtubule organization by the centrosome (compare Figure 1D to 1E), a phenotype consistent with that observed in *spd-2* mutants (O'Connell et al., 2000).

We PCR amplified the F32H2.3 genomic sequence from three *spd-2* mutants and sequenced the amplification products. All three mutants possessed a missense mutation within the F32H2.3 open reading frame, confirming the molecular identity of the *spd-2* gene (Figure 2). To determine the gene structure, we sequenced three cDNA clones. Except for small differences at their termini, all three clones were identical in sequence. The longest clone was 2623 bp in length, in good agreement with the size of *spd-2* message as measured by Northern analysis (data not shown). The *spd-2* gene contains eight exons and encodes a protein of 824 amino acids with a calculated molecular mass of 91.5 kDa (Figure 2A). Analysis of the protein sequence revealed that three regions within SPD-2 have the potential to form coiled coils: amino acids 66–82, 111–131, and 302–324 (Figure 2B). We performed BLAST analysis and identified a putative ortholog from the related nematode *C. briggsae* (Figure 2A) (Stein et al., 2003). Surprisingly, these two proteins share only 42% identity (and 59% similarity), indicating that they rapidly evolved following divergence of the two species. Interestingly, despite the degree of sequence divergence, the putative coiled-coil domain at 302–324 is conserved as are all three amino acid residues affected by mutation. SPD-2 also possesses 23% identity and 39% similarity to an extended region of SPAPB15E9.01c, a *Schizosacchromyces pombe* protein of unknown function (data not shown).

SPD-2 Localizes to Centrosomes

The failure of centrosome components to localize properly in *spd-2* mutants suggests that SPD-2 itself might localize to the centrosome. To address this question, we generated affinity-purified SPD-2 antibodies and used them to stain fixed specimens. We found that SPD-2 not only associates with centrosomes, but it does so at nearly all of the developmental stages examined. In the hermaphrodite gonad, SPD-2 localizes as discrete perinuclear foci in the mitotic portion of the germline (Figure 3A). These foci were also evident during the early stages of oogenesis but were absent in mature oocytes. In contrast, mature sperm retained these SPD-2 foci with each male gamete containing a single dot adjacent to the nucleus (Figure 3B). Similarly, in meiotic stage embryos, a single SPD-2-positive dot was observed next to the male pronucleus (Figure 3C). In slightly older embryos, one or two perinuclear foci of SPD-2 staining were observed (Figure 3D). The intensity of the foci increased with the age of the embryos and at mitosis both spindle poles were brightly stained (Figures 3E–3F). As embryos progressed through anaphase (Figure 3G) and telophase (Figure 3H), the intensity of staining gradually diminished. Careful examination of the staining pattern at this stage revealed a diffuse area of SPD-2 material centered on one or two very bright dots. To determine if these central dots corresponded to the position of centrioles, we examined SPD-2 distribution in a strain expressing a GFP-tagged version of the centriole marker SAS-4 and found that the SPD-2 and SAS-4-positive dots coincided (Figures 3K–3M). Given this result and the localization pattern of SPD-2 in sperm—which contain a centriole pair but lack obvious PCM—we believe that SPD-2 localizes to both centrioles as well the pericentriolar region.

Centrosome staining was also evident in older embryos (Figures 3I and 3J) and SPD-2-positive puncta were seen in young larvae (data not shown), suggesting that SPD-2 is present at the centrosome throughout the entire life cycle. SPD-2 staining, however, was not restricted to the centrosome. We also noticed that varying amounts of SPD-2 were present in the cytoplasm

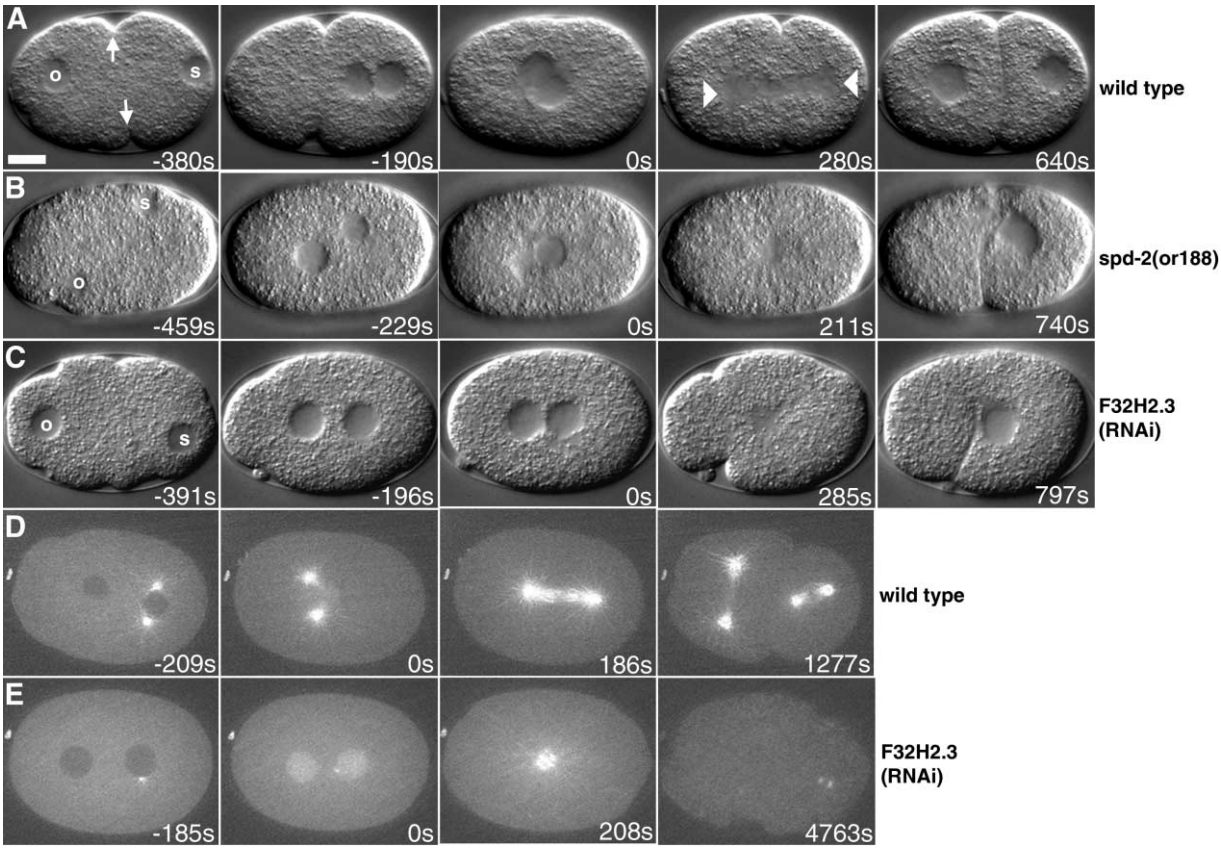

Figure 1. RNAi of F32H2.3 Phenocopies *spd-2* Mutations

(A–C) Time-lapse DIC images of wild-type (A), *spd-2(or188)* (B), and F32H2.3 (RNAi) (C) embryos. Unless indicated otherwise, in all figures embryos are oriented with anterior to left and time is specified relative to nuclear envelope breakdown. From left to right in each series: early pronuclear migration, late pronuclear migration, nuclear envelope breakdown, first mitosis, second interphase. In each series, the initial position of the oocyte (o) and sperm (s) pronucleus is indicated. In wild-type embryos, a pseudocleavage furrow (arrows) transiently appears during pronuclear migration (−380 s) and the pronuclei meet at the posterior (−190 s). In both *spd-2* mutants and F32H2.3 (RNAi) embryos, the pseudocleavage furrow is absent and the pronuclei meet near the center. The bipolar spindle (arrowheads) seen in wild-type embryos (280 s) is absent in both *spd-2(or188)* and F32H2.3 (RNAi) embryos. Bar, 10 μm.

(D and E) Time-lapse images of wild-type (D) and F32H2.3 (RNAi) (E) embryos expressing GFP–α-tubulin. Each image is a projection of three focal planes. For the wild-type, stages shown are from left to right: late pronuclear migration, nuclear envelope breakdown, first mitosis, and second mitosis. For F32H2.3 (RNAi) embryo, stages shown are from left to right: late pronuclear migration, nuclear envelope breakdown, first mitosis, and late stage mitosis. Note the presence of only two asters in the late stage embryo (4763 s).

and nuclei of oocytes and embryos (data not shown). As RNAi of *spd-2* eliminated staining of all subcellular structures (data not shown), we conclude that the staining pattern is specific.

To confirm our immunofluorescence results, we generated a transgenic line expressing GFP–SPD-2. Like the endogenous protein, GFP–SPD-2 localized to centrosomes throughout the cell cycle (Figures 3N–3T). GFP fluorescence was first detected as one or two small foci associated with the male pronucleus (Figure 3N). The size and intensity of these foci increased as the cell cycle progressed and peaked during mitosis (Figures 3O–3R). As in the case of fixed specimens, fluorescence intensity diminished by telophase, leaving behind two small brightly stained dots (Figure 3S). These two dots persisted into the next cell cycle when once again fluorescence intensity gradually increased as the cells progressed toward mitosis (Figure 3T). As with immunofluorescence, we detected weak localization of SPD-2 to nuclei. We conclude that SPD-2 is a nuclear and centrosome protein and that the levels of SPD-2 at the centrosome correlate with the microtubule-organizing capacity.

SPD-2 Requires Aurora Kinase and Cytoplasmic Dynein for Efficient Localization to the Centrosome

To investigate the mechanism whereby SPD-2 is recruited to the centrosome, we analyzed SPD-2 localization in embryos deficient in various centrosome/cytoskeletal components. We first determined if SPD-2 requires microtubules to associate with the centrosome by treating newly fertilized embryos with nocodazole to disrupt microtubules during the process of centrosome maturation. Embryos were then fixed and stained for SPD-2. Despite a nearly complete loss of tubulin polymer, SPD-2 still localized to the centrosome (Figure 4B). To more carefully determine if loss of microtubules had any

A

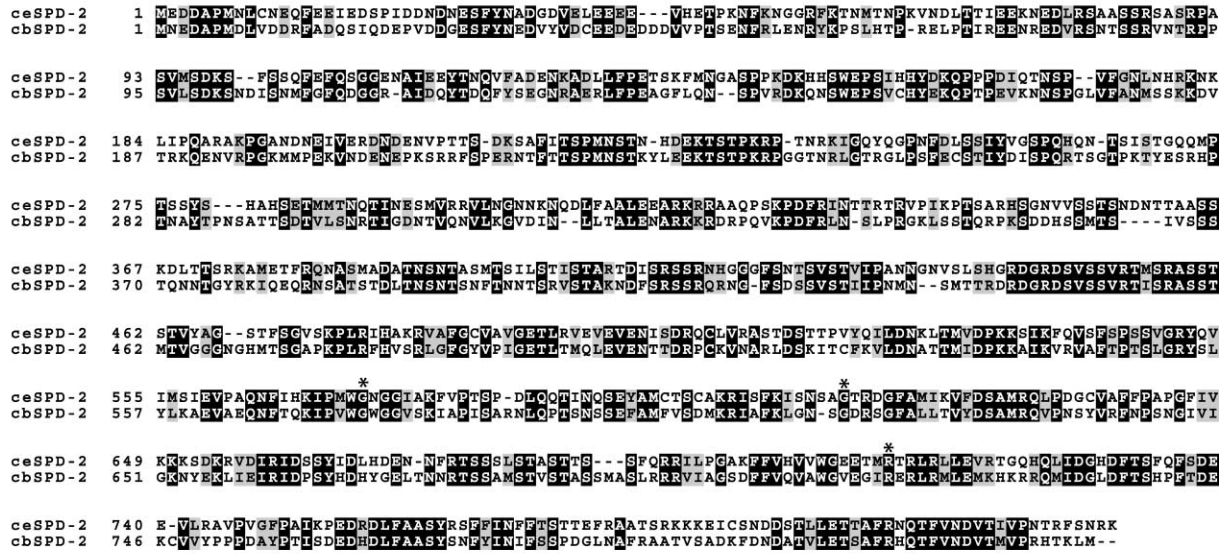

B

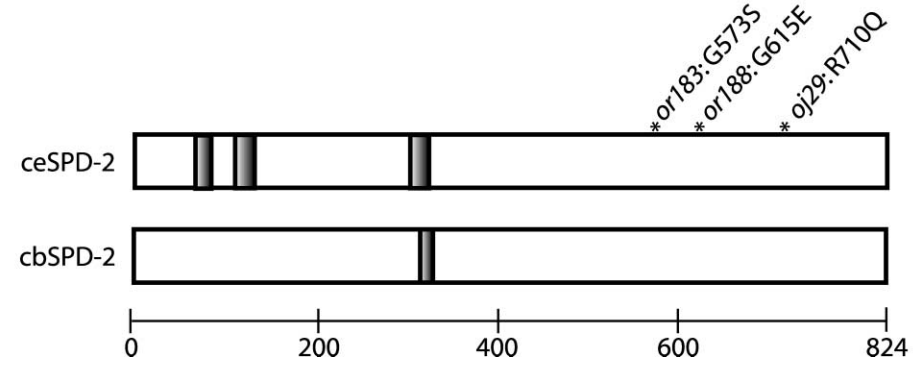

Figure 2. *spd-2* Encodes a Protein with Three Predicted Coiled-Coil Domains

(A) Alignment of *C. elegans* and *C. briggsae* SPD-2 proteins. Identical residues are shown in solid and similar residues are shaded. The full-length *spd-2* cDNA sequence (Accession number: AY340594) can be obtained from GenBank.

(B) Schematic of *C. elegans* and *C. briggsae* SPD-2 proteins showing positions of coiled-coil domains (shaded) and mutations.

effect on SPD-2 localization, we measured fluorescence intensity at the centrosome in treated and untreated embryos. To minimize variability due to age, we compared only those embryos in late prophase and found that nocodazole-treated embryos possessed wild-type levels of SPD-2 at the centrosome (Figure 4H). Next, we tested several factors implicated in centrosome dynamics. The *C. elegans* Aurora-A ortholog is encoded by the *air-1* gene (Schumacher et al., 1998). We treated wild-type hermaphrodites with double-stranded *air-1* RNA to block expression of Aurora-A and immunolocalized SPD-2 within the resulting progeny. While loss of Aurora-A expression led to defects in the microtubule network as previously described (Hannak et al., 2001; Schumacher et al., 1998), all of the one-cell embryos examined (n = 29) contained detectable, albeit lower, levels of SPD-2 at the centrosome (Figure 4C). Fluorescence intensity measurements made on embryos in late prophase indicated that centrosomes in *air-1*(RNAi) embryos possessed half the amount of SPD-2 as wild-type embryos (Figure 4H). There was, however, a large variation in the amount of centrosomal SPD-2 remaining with some *air-1(RNAi)* embryos exhibiting as little as 20% of the wild-type level. Thus, Aurora-A appears to play an important role in recruiting SPD-2 to the centrosome. We also detected a decrease in centrosome-associated SPD-2 in cytoplasmic dynein heavy chain (*dhc-1*) mutants. All one-cell *dhc-1(or195)* embryos examined (n = 23) possessed reduced SPD-2 staining at the centrosome, and fluorescence intensity measurements made on those *dhc-1(or195)* embryos in late prophase revealed that the mutants possessed only 44% of the wild-type level (Figures 4D and 4H). To determine if the localized fraction of SPD-2 in *dhc-1(or195)* mutants was due to residual dynein activity, we performed RNAi of *dhc-1* in the *dhc-1(or195)* mutant background. Although we observed that *dhc-1(or195 + RNAi)* embryos exhibited more severe microtubule defects than *dhc-1(or195)* embryos, we did not detect a further decrease in centrosomal SPD-2 levels (Figure 4H). Thus, SPD-2 localization

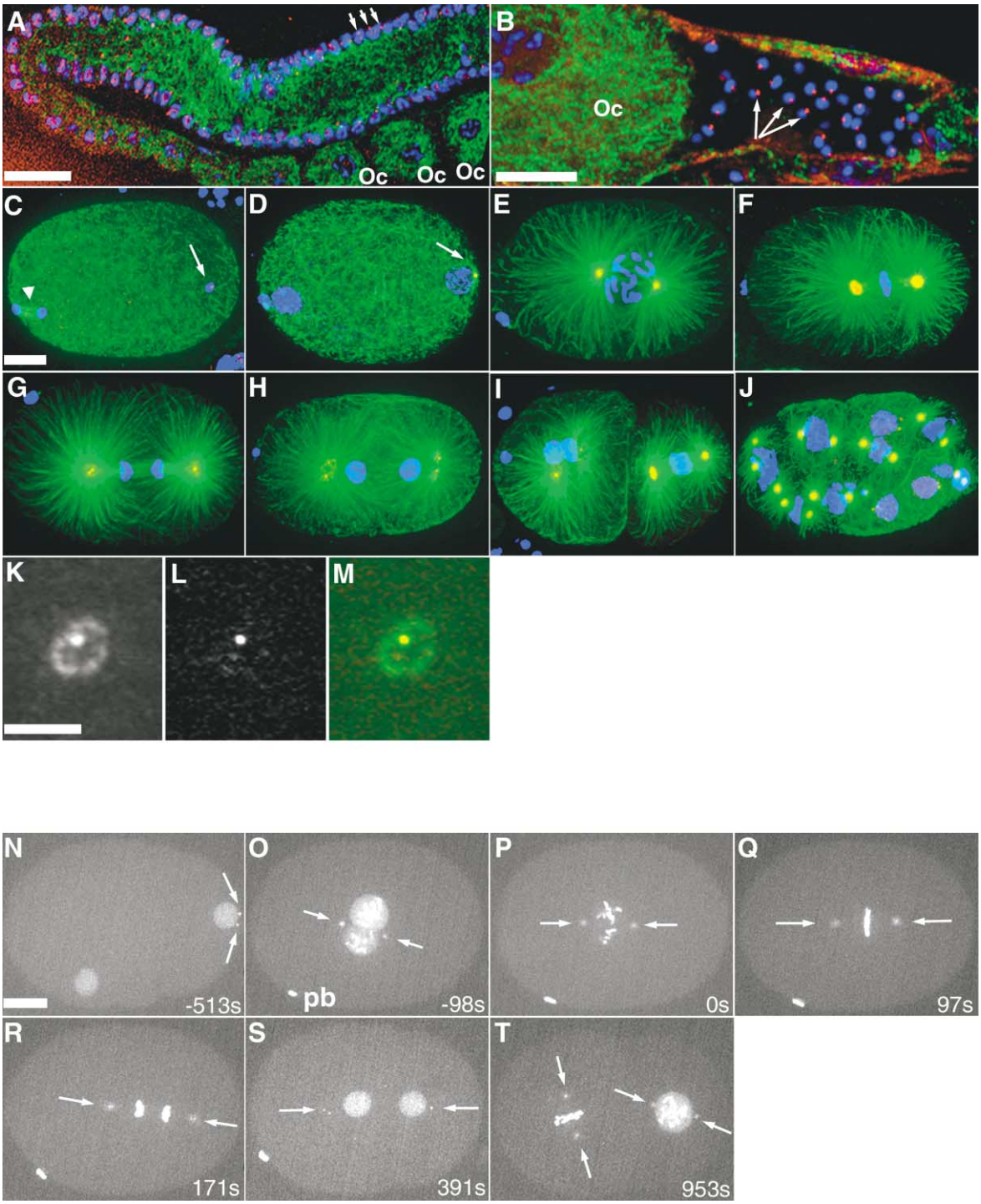

Figure 3. SPD-2 Is a Centrosome Component

(A–J) Wild-type gonads and embryos stained for SPD-2 (red—sometimes appears yellow due to overlap with green channel), microtubules (green), and DNA (blue). Each image is a projection of multiple focal planes. SPD-2 concentrates in perinuclear foci (arrows) in the distal portion of the hermaphrodite germline (A). Such foci are absent in oocytes (Oc). Bar, 25 μm. SPD-2 also concentrates as a single focus in sperm (B). Sperm nuclei (arrows) are visible to the right of a mature oocyte. Bar, 25 μm. In one-cell embryos, SPD-2 is present at the centrosome during meiosis (C), interphase (D), prophase (E), metaphase (F), anaphase (G), and telophase (H). In (C), a meiotic spindle (arrowhead) is visible, and in (C) and (D), the sperm pronucleus and associated centrosome are indicated by arrows. SPD-2 is also present at the two-cell stage (I) and in multicellular embryos (J). Bar in (C) is 10 μm and applies to (C)–(J).

(K–M) SPD-2 localizes to both PCM and centrioles. Localization of SPD-2 (K) and the centriole marker GFP–SAS-4 (L) within the same centrosome. The merged image (M) shows that a portion of SPD-2 is closely associated with the centrioles. Bar, 5 μm.

(N–T) Time-lapse confocal images of a strain coexpressing GFP–SPD-2 and GFP–Histone. GFP–SPD-2, indicated by arrows, is detected at centrosomes which are initially found in close association with the male pronucleus (N), and later with the two conjoined pronuclei (O). During each mitosis, GFP–SPD-2 localizes to the spindle poles (P–T). A polar body (pb) labeled by the GFP–Histone marker is visible in (O)–(S). Bar, 10 μm.

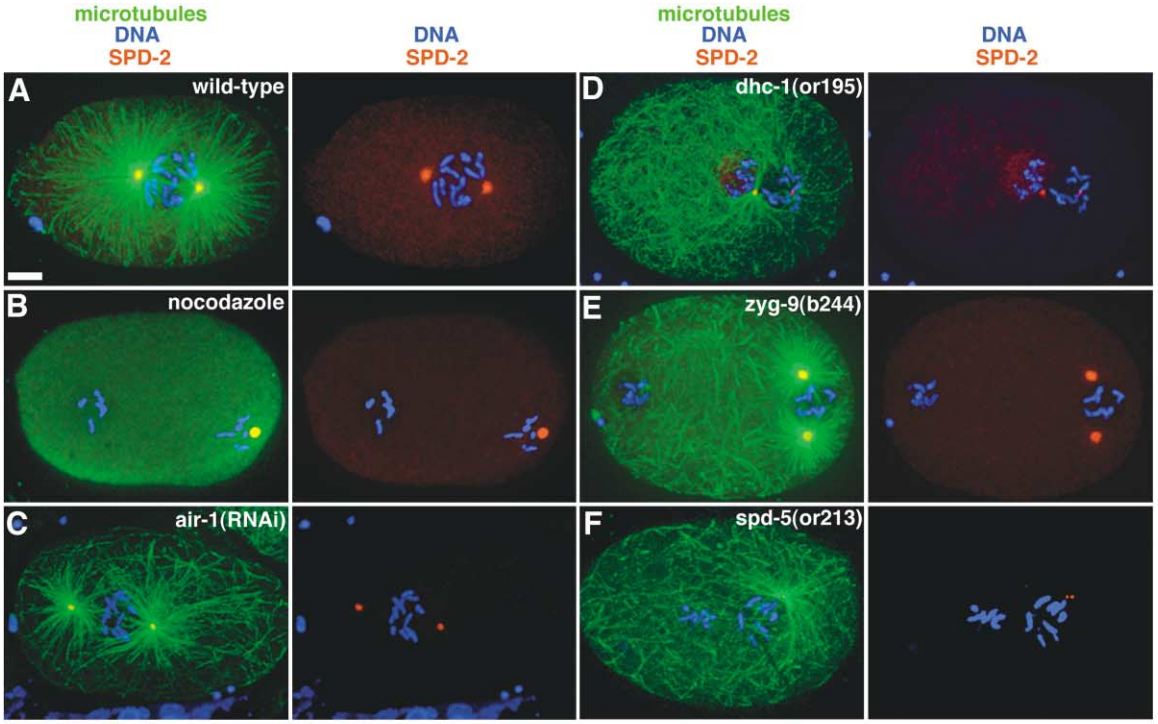

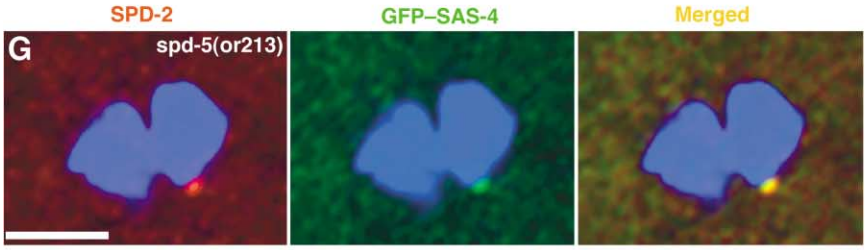

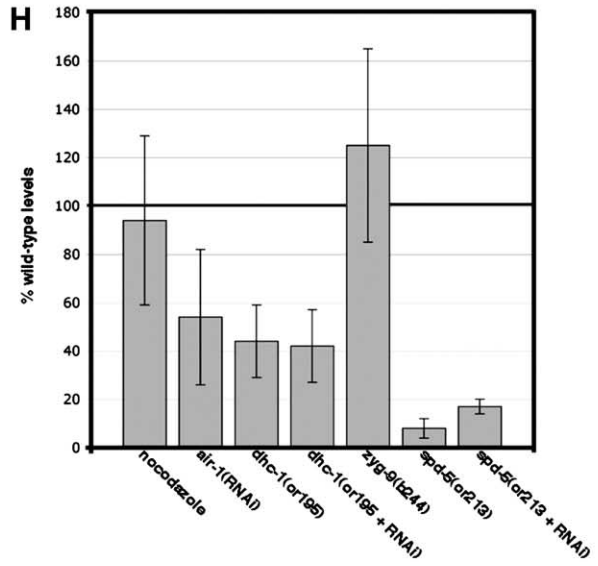

Figure 4. Requirements for SPD-2 Localization

(A–F) Embryos in late prophase stained for SPD-2 (red), microtubules (green), and DNA (blue). For each specimen, the left-hand panel shows the triple-stained image and the right-hand panel shows SPD-2 and DNA staining. Shown are comparable images of a wild-type embryo (A),

to the centrosome is at least partially dependent on cytoplasmic dynein. In contrast, we did not detect a loss of centrosome-associated SPD-2 in embryos lacking ZYG-9, an XMAP215 homolog (Figure 4E, n = 27) (Matthews et al., 1998). In fact, fluorescence intensity measurements made on late prophase embryos indicated that *zyg-1(b244)* mutants possessed slightly elevated levels of SPD-2 at the centrosome (Figure 4H).

SPD-5 Is Required for Association of SPD-2 with the PCM but Not the Centrioles

Recently, Hamill et al. (2002) reported that the SPD-5 protein is required for maturation and localizes to centrosomes in a manner that is at least partially dependent on SPD-2. To determine if SPD-5 and SPD-2 are mutually dependent on each other for localization to the centrosome, we examined SPD-2 localization in *spd-5* mutant embryos. In all *spd-5(or213)* embryos examined (n = 33), the level of SPD-2 at the centrosome was dramatically reduced (Figure 4F). We found that during late prophase, centrosomes in *spd-5(or213)* embryos possessed less than 10% of the wild-type level of SPD-2 (Figure 4H). The SPD-2 remaining at the centrosome in *spd-5(or213)* mutants was not reduced further in *spd-5(or213 + RNAi)* embryos (Figure 4H), indicating that a fraction of SPD-2 localizes independently of SPD-5. Interestingly, the SPD-2 remaining at the centrosome localized as one or two small bright foci, a pattern reminiscent of centriole staining. As SPD-5 appears to localize to the PCM only and not to centrioles (Hamill et al., 2002), it was possible that loss of SPD-5 affected only the pericentriolar localization of SPD-2. To investigate this possibility, we examined the distributions of endogenous SPD-2 and the GFP–SAS-4 protein in the *spd-5(or213)* mutant. We found that the residual SPD-2 staining was essentially limited to the domain of GFP–SAS-4 fluorescence (Figure 4G), indicating that centriole-associated SPD-2 localizes in the absence of SPD-5. In support of this, we have found that SPD-2 localizes normally in *spd-5(or213)* sperm (data not shown). Ultrastructural analysis indicates that sperm contain a centriole pair but no associated PCM (for example, see O'Connell et al., 2001). Thus, the localized SPD-2 observed in sperm is likely in close association with the centrioles. We conclude that SPD-5 is required to recruit SPD-2 to the PCM but does not appear to be important for its association with centrioles.

SPD-2 Acts Early in the Maturation Pathway

Previously, we determined that SPD-2 is required for centrosomes to recruit γ-tubulin and ZYG-9 (O'Connell et al., 2000). To build a morphogenetic pathway of centrosome maturation, we will ultimately need to determine how loss of each component affects assembly of the overall structure. With this in mind, we sought to determine how the loss of SPD-2 affects the localization of other centrosome components. We first investigated whether SPD-2 is required for localization of Aurora-A. In wild-type embryos, Aurora-A concentrates at centrosomes and the minus ends of microtubules (Figure 5A and Schumacher et al., 1998). In the *spd-2(or188)* mutant, however, localization of Aurora-A to the centrosome was nearly undetectable (Figure 5B) with only 3% of wild-type levels being present in late prophase centrosomes (Figure 5G). As *or188* is unlikely to be a null mutation, we also analyzed AIR-1 localization in *spd-2(or188 + RNAi)* embryos. Under these conditions of reduced *spd-2* activity, only 0.5% of AIR-1 localized properly (Figure 5G). Thus, SPD-2 is required for localization of Aurora-A. We next examined the distribution of SPD-5 in the *spd-2(or188)* mutant. We found that, consistent with the results of Hamill et al. (2002), SPD-5 levels at the centrosome decreased in the absence of functional SPD-2 (compare Figures 5C and 5D). To quantify this effect, we performed fluorescence intensity measurements and found that SPD-5 staining of *spd-2(or188)* centrosomes was only 1.7% of wild-type levels (Figure 5G). We conclude that SPD-5 and SPD-2 are dependent on one another for localization to the PCM. Finally, we investigated whether Polo-like kinase requires SPD-2 for localization. The *plk-1* gene encodes a *C. elegans* Polo-like kinase that localizes to centrosomes and is essential for normal oocyte and embryonic development (Figure 5E and Chase et al., 2000). Interestingly, we found that PLK-1 was completely absent from centrosomes in the *spd-2(or188)* mutant (Figure 5F). In fact, when we carefully examined PLK-1 staining during late prophase, we could not detect centrosome staining above background in any of the *spd-2(or188)* mutants examined (Figure 5G). Thus, SPD-2 is required for localization of all centrosome components so far tested and appears to act near the top of a hierarchy in the centrosome maturation pathway.

SPD-2 Interacts Genetically with SPD-5 and Dynein Heavy Chain

In the course of our studies on SPD-2, we noticed a genetic interaction with SPD-5. Both the *spd-2(oj29)* and *spd-5(or213)* mutations are recessive at the restrictive temperature of 25°C (Hamill et al., 2002; O'Connell et al., 2000). However, we found that over half of the eggs produced by hermaphrodites heterozygous for both alleles failed to hatch at 25°C (Table 1). Although rare, this

a nocodazole-treated embryo (B), an *air-1*(RNAi)-treated embryo (C), a *dhc-1(or195)* embryo (D), a *zyg-9(b244)* embryo (E), and a *spd-5(or213)* embryo (F). Note that nocodazole treatment (B) blocks pronuclear migration. Bar, 10 μm.

(G) Colocalization of SPD-2 (red) and GFP–SAS-4 (green) in a *spd-5(or213)* mutant. High magnification view of *spd-5(or213)* embryo showing DNA (blue) and residual SPD-2 staining (left panel) or DNA and GFP–SAS-4 (middle panel). The merged image (right panel) shows that SPD-2 remaining in the *spd-5* mutant is closely associated with the centriole. Bar, 5 μm.

(H) Quantification of centrosomal SPD-2 levels in embryos lacking various centrosome components. For each mutant/condition, the average value ± the standard deviation is shown. The number of late prophase MTOCs/embryos surveyed is as follows: 15 MTOCs in 8 embryos for nocodazole treatment; 33 MTOCs in 15 embryos for *air-1(RNAi)*; 14 MTOCs in 7 embryos for *dhc-1(or195)*; 28 MTOCs in 14 embryos for *dhc-1(or195 + RNAi)*; 14 MTOCs in 7 embryos for *zyg-9(b244)*; 12 MTOCs in 6 embryos for *spd-5(or213)*; 12 MTOCs in 6 embryos for *spd-5(or213 + RNAi)*.

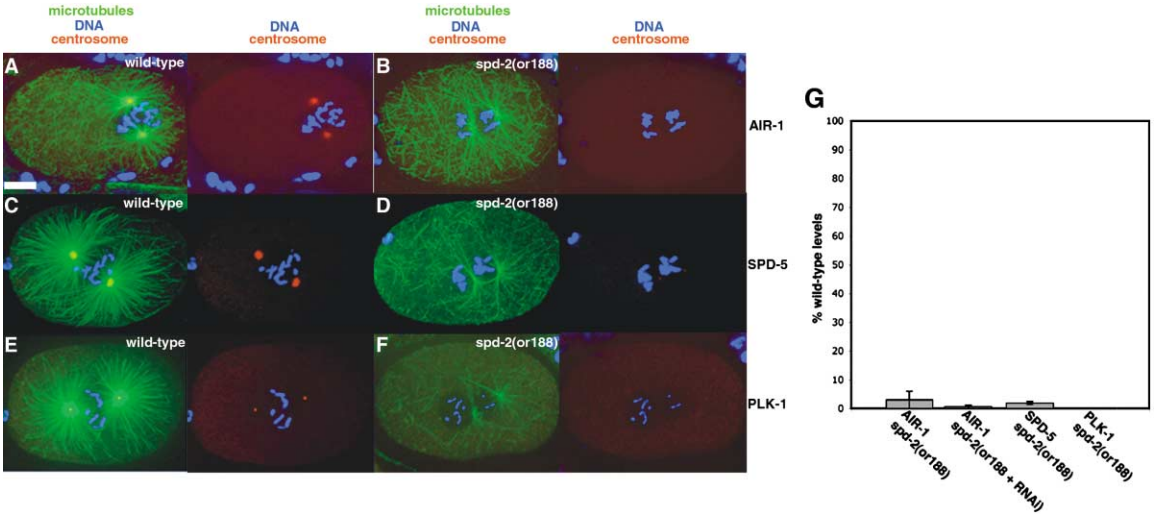

Figure 5. SPD-2 Is Required for Localization of AIR-1, SPD-5, and PLK-1

(A–F) Embryos in late prophase stained for centrosome components (red), microtubules (green), and DNA (blue). For each set of panels, the triple-stained image is shown on the left while the corresponding DNA and centrosome staining is shown on the right. Shown are comparable images of the following: wild-type (A) and *spd-2(or188)* (B) embryos stained for AIR-1; wild-type (C) and *spd-2(or188)* (D) embryos stained for SPD-5; and wild-type (E) and *spd-2(or188)* (F) embryos stained for PLK-1. Bar, 10 μm.

(G) Quantification of centrosomal protein levels in embryos lacking SPD-2. For each measurement, the average value ± the standard deviation is shown. The number of late prophase MTOCs/embryos surveyed is as follows: 10 MTOCs in 5 embryos for AIR-1/*spd-2(or188)*; 11 MTOCs in 6 embryos for AIR-1/*spd-2(or188 + RNAi)*; 12 MTOCs in 7 embryos for SPD-5/*spd-2(or188)*; 24 MTOCs in 12 embryos for PLK-1/*spd-2(or188)*.

type of interaction is indicative of genes that have a common function. A similar genetic interaction has been described for *spd-5* and *dhc-1* (Hamill et al., 2002). Thus, we decided to test for an interaction between *spd-2(oj29)* and the recessive mutation *dhc-1(or195)*. When hermaphrodites heterozygous at both loci were allowed to lay eggs at 25°C, all of the progeny failed to hatch (Table 1). Thus, a mutation in any one of these genes exhibits strong nonallelic noncomplementation with a mutation in either one of the other two genes, indicating that SPD-2, SPD-5, and DHC-1 function together to regulate centrosome maturation. To investigate the specificity of these interactions, we tested the *spd-2(oj29)* mutation for nonallelic noncomplementation with mutant alleles of two other genes with centrosome-related functions. Significant embryonic lethality was not observed among the progeny of hermaphrodites heterozygous for both *spd-2(oj29)* and *zyg-9(b244)* (Table 1). We also failed to detect an interaction between *spd-2* and *tbg-1*, the gene encoding γ-tubulin. The level of lethality

Table 1. Genetic Interactions among Components of the Centrosome Maturation and Duplication Pathways

Parent	Percent Lethality among Offspring (25°C)	N
+ / *spd-5(or213)*[b] ; *dpy-5(e61)* / + ; *spd-2(oj29)*[a] / +	56	145
+ / *dhc-1(or195)*[c] ; *dpy-5(e61)* / + ; *spd-2(oj29)* / +	100	186
dpy-5(e61) / + ; *spd-2(oj29)* / + ; *tbg-1 (t1465)*[d] / +	7.2	445
dpy-5(e61) / + ; *spd-2(oj29)* / + ; *zyg-9 (b244)*[e] / +	6.4	173
dpy-5(e61) / + ; *spd-2(oj29)* / + ; *zyg-1 (oj7)*[f] / +	76	243
spd-5(or213) / + ; *zyg-1 (oj7)* / +	86	310
dhc-1(or195) / + ; *zyg-1 (oj7)* / +	84	316

[a] Offspring of *dpy-5(e61) spd-2(oj29)*/++ hermaphrodites exhibit 0.6% lethality (n = 503)
[b] Offspring of *spd-5(or213)*/+ hermaphrodites exhibit 10% lethality (Hamill, 2002)
[c] Offspring of *dhc-1(or195)*/+ hermaphrodites exhibit 26% lethality (n = 424)
[d] Offspring of *tbg-1(1465)*/+ hermaphrodites exhibit 6.0% lethality (n = 235)
[e] Offspring of *zyg-9(b244)*/+ hermaphrodites exhibit 6.4% lethality (n = 280)
[f] Offspring of *zyg-1(oj7)*/+ hermaphrodites exhibit 10% lethality (O'Connell, 1998)

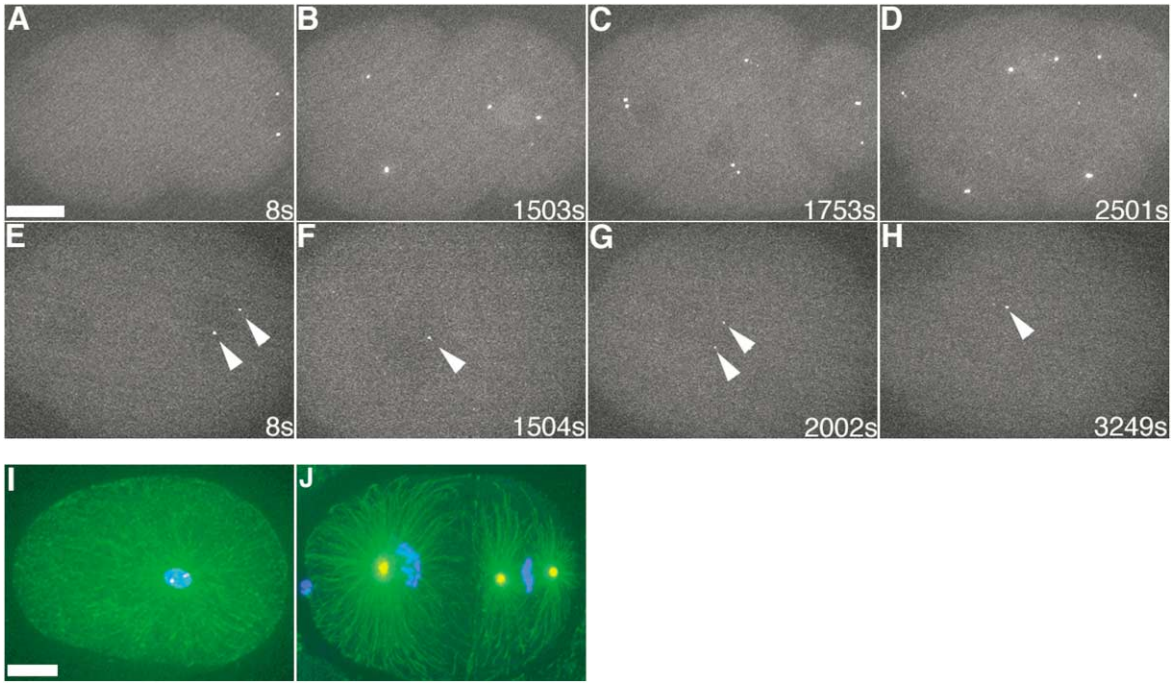

Figure 6. *spd-2* Is Required for Centrosome Duplication and Genetically Interacts with Maturation and Duplication Genes

(A–H) Four-dimensional time-lapse imaging of wild-type (A–D) and *spd-2(RNAi)* (E–H) embryos expressing GFP–SAS-4. Each image is a projection of 14 focal planes. Time is specified relative to the first frame. Wild-type control embryos exhibit a regular doubling of GFP–SAS-4 foci each cell cycle. In *spd-2(RNAi)* embryos (E–H), no more than one or two foci (arrowheads) are detectable within the embryo each cell cycle. The intensity of these foci is less than control embryos. Bar, 10 μm.

(I) Embryo produced by *spd-5(or213)* +/+ *spd-2(oj29)* mother stained for microtubules (green), SPD-2 (red), and DNA (blue). Bipolar spindle assembly has failed. Instead, two immature centrosomes and DNA are at the center of a radial array of microtubules. This phenotype is identical to that observed in both *spd-2(oj29)* (O'Connell et al., 2000) or *spd-5(or213)* homozygotes (Hamill et al., 2002). Bar, 10 μm, applies to (I) and (J).

(J) Embryo produced by *spd-2(oj29)/+ ; zyg-1(oj7)/+* mother stained for microtubules (green), SPD-2 (red), and DNA (blue). Bipolar spindle assembly has failed in the cell on the left. Instead, a single mature centrosome organizes a monopolar spindle. This phenotype is similar to that observed in *zyg-1(oj7)* homozygotes (O'Connell et al., 2001).

among the progeny of hermaphrodites heterozygous for both *spd-2(oj29)* and *tbg-1(t1465)* was small and not significantly different from that measured for *tbg-1(t1465)* heterozygotes (Table 1). We conclude that the interactions between *spd-2*, *spd-5*, and *dhc-1* are specific and indicate a commonality of function among this subset of centrosome factors.

We next investigated the cytological basis for the lethality incurred by the progeny of such double heterozygotes. Embryos from *spd-5(or213)* +/+ *spd-2(oj29)* mothers were fixed and stained for microtubules, SPD-2, and DNA. Examination revealed centrosome maturation defects essentially identical to those observed in *spd-2* and *spd-5* mutants (Figure 6I). In such embryos, two separated centrosomes were apparent but each accumulated only trace amounts of SPD-2 and spindle assembly failed (Figure 6I). We observed similar defects among the progeny of *dhc-1(or195)* +/+ *spd-2(oj29)* mothers (data not shown), and, consistent with these findings, Hamill et al. (2002) reported spindle assembly defects among the progeny of *spd-5(or213)* +/+ *dhc-1(or195)* mothers. Thus, lethality among the progeny of double heterozygotes is due to defects in centrosome maturation, consistent with the idea that SPD-2 functions in concert with SPD-5 and cytoplasmic dynein to regulate this process.

SPD-2 Functions in the Centrosome Duplication Pathway

During these studies, we noticed that embryos lacking SPD-2 typically arrested as one-cell embryos with no more than two small asters. For instance, when we performed *spd-2* RNAi on worms expressing GFP–α-tubulin, we could not detect more than two organizing centers even after multiple cell cycles had passed (Figure 1E). This was in sharp contrast to other mutants such as *spd-5(or213)* and *dhc-1(or213)* which arrest as one-cell embryos but generate multiple (albeit abnormal) MTOCs as they age (data not shown). To investigate this phenotype further, we examined centriole duplication in the GFP–SAS-4-expressing strain following RNAi of *spd-2*. In time-lapse images of wild-type control embryos, we clearly detected a doubling of GFP–SAS-4-labeled centrioles each cell cycle (Figures 6A–6D). In contrast, centriole doubling did not occur in the *spd-2(RNAi)* embryos. As in control embryos, newly fertilized *spd-2(RNAi)* embryos contained two GFP–SAS-4-positive dots associated with the sperm pronucleus (Figure 6E). Interestingly, the fluorescence intensity of these foci was diminished relative to the untreated controls. Nonetheless, we could still reliably detect these foci and found that additional centrioles were not generated in the absence of SPD-2 (Figures 6E–6H). This was not

due to a failure of cell cycle progression, since loss of SPD-2 does not affect this process (O'Connell et al., 1998). As SAS-4 is a component of centrioles (Kirkham et al., 2003) and new GFP–SAS-4-positive foci are not generated in the *spd-2(RNAi)* embryos, we conclude that SPD-2 is required for centriole duplication.

If *spd-2* functions in duplication, we reasoned that it might exhibit a genetic interaction with *zyg-1*, a gene encoding an essential regulator of duplication (O'Connell et al., 2001). Intriguingly, we found that *spd-2* and *zyg-1* exhibit a potent genetic interaction; mothers heterozygous for both *spd-2(oj29)* and *zyg-1(oj7)* produce predominantly dead embryos (Table 1), indicating that SPD-2 and ZYG-1 function in a common pathway. Unexpectedly, however, we also found that *spd-5* and *dhc-1* each exhibit a similar genetic interaction with *zyg-1* (Table 1). Mothers heterozygous for both *zyg-1(oj7)* and *spd-5(or213)* and mothers heterozygous for both *zyg-1(oj7)* and *dhc-1(or195)* produce mostly dead progeny. To explore the basis for these embryonic lethal phenotypes, we examined the progeny of all three double heterozygotes by immunofluorescence microscopy. The progeny of *spd-2(or188)/+ ; zyg-1(oj7)/+* mothers were unique in that they exhibited monopolar spindles (Figure 6J). These monopolar spindles were organized by a single mature organizing center and were similar in appearance to the monopolar spindles of *zyg-1(oj7)* homozygotes (O'Connell et al., 2001). Monopolar spindles were not observed, however, among the progeny of *spd-5(or213)/+ ; zyg-1(oj7)/+* and *dhc-1(or195)/+ ; zyg-1(oj7)/+* hermaphrodites, indicating that while *zyg-1*, *spd-5*, and *dhc-1* seem to cooperate to carry out some essential cellular process, this process is not centrosome duplication. In fact, our cytological analysis suggests that *spd-5(or213)/+ ; zyg-1(oj7)/+* and *dhc-1(or195)/+ ; zyg-1(oj7)/+* embryos die of cytokinesis failures (data not shown). Only one activity each has been ascribed to *spd-5* (centrosome maturation) and *zyg-1* (centrosome duplication), and thus our data suggest the exciting possibility that additional functions exist for these genes and that these functions can be unmasked through genetic analysis.

We note that the centrosome phenotype of *spd-2(or188)/+ ; zyg-1(oj7)/+* animals is quite distinct from the centrosome phenotype observed among the offspring of *spd-5(or213) +/+ spd-2(oj29)* mothers (Figure 6I). Specifically, in *spd-2(oj29)/+ ; zyg-1(oj7)/+* embryos we observed unreplicated centrosomes with a normal complement of SPD-2 (Figure 6J), whereas in *spd-5(or213) +/+ spd-2(oj29)* offspring we observed duplicated centrosomes associated with abnormally low levels of SPD-2 (Figure 6I). These distinct phenotypes indicate that the causes underlying the *spd-2-spd-5/dhc-1* and *spd-2-zyg-1* interactions are fundamentally different.

Discussion

SPD-2 functions in two processes essential to centrosome function: maturation and duplication. In the absence of SPD-2 activity, the paternally inherited centriole pair fails to accumulate the normal complement of PCM components. This results in two immature MTOCs with relatively few microtubules and, subsequently, a failure of mitotic spindle assembly. These phenotypes are shared by embryos lacking various components of the maturation pathway (Hamill et al., 2002; Hannak et al., 2001, 2002; Schumacher et al., 1998; Strome et al., 2001). *spd-2* mutants also show defects in centrosome duplication; while two MTOCs arise during the first cell cycle in embryos lacking SPD-2, additional centrosomes are not generated during later cycles. This is in sharp contrast to *air-1(RNAi)* and *spd-5(or213)* embryos which arrest with multiple MTOCs (data not shown). An obvious possibility suggested by our work is that centriole-associated SPD-2 is involved in centrosome duplication and PCM-localized SPD-2 is involved in microtubule nucleation. Consistent with this hypothesis, we have found that *spd-5* mutations, which inhibit maturation, only affect SPD-2 association with the PCM.

SPD-2 appears to function in concert with SPD-5, Aurora-A kinase, and cytoplasmic dynein early in the maturation pathway. Microtubule nucleation at the centrosome is predominantly γ-tubulin dependent in *C. elegans* (Hannak et al., 2002), and SPD-5 (Hamill et al., 2002), Aurora-A (Hannak et al., 2001), and SPD-2 (O'Connell et al., 2000) are all required for γ-tubulin to associate with the PCM. Our data indicate that SPD-2, SPD-5, Aurora-A, and cytoplasmic dynein all act at the same specific step in the pathway. We have found that some degree of interdependency exists between SPD-2 and SPD-5 and between SPD-2 and Aurora-A for localization to the centrosome. We have also determined that cytoplasmic dynein plays an important role in localizing SPD-2 to the centrosome. Finally, we have discovered that *spd-2*, *spd-5*, and *dhc-1* mutations exhibit strong genetic interactions with each other (Table 1 and Hamill et al., 2002). We were unable, however, to detect an interaction between *spd-2* and the γ-tubulin-encoding gene *tbg-1*. Since γ-tubulin is also required for the process of centrosome maturation (Hannak et al., 2002), the genetic interactions seem to suggest a more specific functional connection than participation in a common pathway.

The precise role of SPD-2 in centrosome maturation is not yet clear, but one intriguing possibility is that SPD-2 along with SPD-5 forms part of the centromatrix (Dictenberg et al., 1998; Schnackenberg et al., 1998), an intricate network of 12–15 nm fibers visible in salt-extracted centrosomes. The matrix proper lacks microtubule-nucleating activity but is thought to provide a structural framework that anchors γ-tubulin ring complexes (γ-TuRCs). The γ-TuRCs have a lock washer-like structure and possess microtubule-nucleating and capping activities (Moritz et al., 2000; Oegema et al., 1999; Wiese and Zheng, 2000; Zheng et al., 1995). Thus, by binding γ-TuRCs, the centromatrix provides a localized site of microtubule-organizing activity. One component of the centromatrix in vertebrates is pericentrin, a protein with multiple small coiled-coil domains (Doxsey et al., 1994). SPD-5 also has multiple coiled-coil domains, and it has been suggested that SPD-5 and pericentrin are functionally equivalent (Hamill et al., 2002). This might well be the case, and given that SPD-2 has coiled-coil domains and functionally interacts with SPD-5, SPD-2 might physically interact with SPD-5 to form the *C. elegans* centromatrix.

Where then would Aurora-A fit into this picture? Aurora-A might phosphorylate SPD-2 and/or SPD-5 to regulate centromatrix assembly. As centromatrix is formed, Aurora-A could concentrate at the nascent PCM to further drive maturation, thus providing a positive feedback loop. What role the microtubule-based motor protein dynein might have in this process is unclear, as microtubules are not necessary for localization of SPD-2 (Figure 3) or SPD-5 (Hamill et al., 2002), but, intriguingly, dynein light intermediate chain has been shown to interact with pericentrin in vertebrate cells (Purohit et al., 1999).

The requirement for SPD-2 in centrosome duplication might reflect an essential role in assembly of daughter centrioles. Although we have not yet investigated the duplication defect at an ultrastructural level, the light microscope phenotype is consistent with such a defect. During the first cell cycle of *spd-2* mutant embryos, two clearly separate MTOCs are formed, but additional MTOCs do not arise during subsequent divisions. This is identical to the events that occur when daughter centriole formation is blocked by *zyg-1* mutations or *sas-4* RNAi (Kirkham et al., 2003; Leidel and Gonczy, 2003; O'Connell et al., 2001) and results from a one-time splitting of the sperm-donated centriole pair to form two centriole singlets. Because daughter centriole assembly is blocked, two and only two MTOCs are formed. Our finding that *spd-2* and *zyg-1* interact genetically provides further evidence for a role for SPD-2 in assembly of daughter centrioles. It should be emphasized that while we have uncovered many such interactions between genes with centrosome-related functions, only the *spd-2-zyg-1* interaction was found to be associated with a monopolar spindle phenotype, indicative of a centrosome duplication defect.

How might SPD-2 function in both centrosome maturation and duplication? One possibility is that SPD-2 has two distinct molecular activities. If so, these might be separable by mutation, but so far all mutations analyzed (as well as RNAi) produce essentially identical phenotypes. Another possibility is that SPD-2 only directly participates in one of these processes and its effect on the other is indirect. For instance, SPD-2 might only be required for assembly of a fully functional centriole. In mammalian cells, centrioles appear required to maintain centrosome integrity and their loss results in dispersal of PCM components (Bobinnec et al., 1998). Thus, the loss of SPD-2 activity could result in incomplete centriole duplication and a failure of these defective centrioles to organize PCM, as has been observed in *C. elegans* embryos partially depleted of SAS-4 (Kirkham et al., 2003). However, unlike SAS-4, SPD-2 localizes to both centrioles and PCM, suggesting it functions in the two processes directly. Thus, our favored hypothesis is that SPD-2 has but one molecular activity that is utilized by both processes. During maturation, SPD-2 functions at some level to recruit the microtubule-nucleating machinery to the PCM, and during duplication SPD-2 might also function to recruit microtubule-nucleating factors to the site of centriole synthesis. One of the factors likely to be recruited is γ-tubulin, which is known to be involved in microtubule nucleation and has more recently been implicated in centrosome duplication (Ruiz et al., 1999; Shang et al., 2002). Previously, we have shown that SPD-2 plays a role in recruiting γ-tubulin to the centrosome (O'Connell et al., 2000). Our present findings that SPD-2 is required for both centrosome maturation and duplication could be explained if SPD-2 were involved in localizing γ-tubulin to the PCM as well as the sites of centriole synthesis.

Experimental Procedures

Nematodes, Strain Maintenance, and Genetics

Worms were maintained using standard techniques (Brenner, 1974). N2 Bristol was the wild-type strain. The following alleles were used: LG1: *dhc-1(or195ts)*, *spd-5(or213ts)*, *dpy-5(e61)*, *spd-2(oj29ts)*, *spd-2(or188ts)*, *spd-2(or183ts)*; LGII: *zyg-1(oj7)*, *zyg-9(b244ts)*; and LGIII: *unc-32(e189)*, *tbg-1(t1465)*, *unc-119(ed3)*. Some mutations were balanced with the rearrangements *hT2* [*bli-4(e937) let-?(h661) qIs48* (*myo-2–GFP pes-10–GFP gut enhancer–GFP*)] (*I;III*) or *qC1* [*dpy-19(e1259) glp-1(q339)*] *III*. We also used the following integrated transgenes: *bsIs2* [*pCK6.1*: *unc-119(+) pie-1*–GFP–*spd-2*], *ojIs2* [*pLM6*: *unc-119(+) pie-1*–GFP–*tba-1*], *ruIs32* [*pAZ132: unc-119(+) pie-1*–GFP–*his-58*] (Praitis et al., 2001), and *isIs20* [*pSL446*: *unc-119(+) pie-1-GFP-sas-4*] (Leidel and Gonczy, 2003). Ts strains were maintained at 16°C except where noted. GFP-expressing lines were grown at 24°C, and all other strains were grown at 20°C. For phenotypic analysis of *spd-2(or188ts)*, adults were shifted to 25°C for 6–8 hr before progeny were analyzed. For all other ts mutants, L4 larvae were shifted to the restrictive temperature overnight and progeny analyzed the next day.

To test for nonallelic noncomplementation, individual matings between males of genotype *spd-5(or213)/+*, *dhc-1(or195)/+*, *zyg-9(b244)/+*, *unc-32 (e189) tbg-1(t1465)/++*, or *zyg-1(oj7)/+* and hermaphrodites of genotype *dpy-5(61) spd-2(oj29)/ hT2* [*qIs48*] were performed at 20°C. For each cross, F1 non-Dpy L4 larvae lacking the pharyngeal GFP fluorescence produced by the *hT2* [*qIs48*] chromosome were placed singly at 25°C. After 24–26 hr, the hermaphrodites were transferred to new plates which were then moved to 20°C. To confirm the genotype of the F1 hermaphrodite, the viable F2 progeny produced on these plates were analyzed for the presence of the paternally donated mutation. The original plates were left at 25°C to allow viable animals to hatch. After an additional 24 hr, these plates were examined and live and dead progeny counted. Interactions between *zyg-1*, *spd-5*, and *dhc-1* were done by mating *zyg-1(oj7)/+* males to *spd-5(or213)* or *dhc-1(or195)* hermaphrodites and analyzing the doubly heterozygous progeny.

Molecular Biology

The F32H2.3 EST clones yk86c9, yk483b10, and yk134g11 were obtained from Yuji Kohara. To construct pCK2.7, the *spd-2* RNAi feeding vector, a 1.3 Kbp BamHI-XmnI restriction fragment of cDNA was cloned between the BglII and SmaI sites of plasmid L4440 (Kamath et al., 2001). The *air-1* feeding vector pCK8.1 was constructed using the primers 5′-GAAGATCTTGAGCGGAAAGGAAAAT ACTG-3′ and 5′-GAAGATCTATTGATTGGCTGTAGAATTATTGCGA-3′ to amplify *air-1* message from the cDNA library pHS1. The amplification product was cut with BglII and cloned into the BglII site of plasmid L4440. A similar approach was used to construct pJM1, the *dhc-1* feeding vector, using primers 5′-GAAGATCTAAGGAA GGAGCTCAACGACA-3′ and 5′-GAAGATCTCCTTTCCTTCCTGGG TCTTC-3′. For pCK6.1, the *pie-1*–GFP–*spd-2* construct, a 3.0 Kbp fragment encoding the entire *spd-2* sequence was amplified from a genomic N2 template using the primers 5′-GGGGACAAGTTTGTA CAAAAAAGCAGGCTTGGAAGATGATGCTCCAATG-3′ and 5′-GGG GACCACTTTGTACAAGAAAGCTGGGTATTACTTTCTATTCGAAAA TCTTG-3′. The gel-isolated product was inserted into the entry vector pDONR201 (Invitrogen) using Gateway Technology per manufacturer's instructions. The resulting entry clone was then used in an LR recombination reaction with the destination vector pID3.01B (gift of Geraldine Seydoux) to create the pCK6.1 bombardment construct. Biolistic transformation was performed as previously described (Praitis et al., 2001).

RNAi was performed using published protocols (Kamath et al., 2001). For sequencing of mutant alleles, amplified genomic DNA served as template. Genomic and cDNA sequencing was performed

at the UW Biotechnology Center on an ABI 377XL sequencer. Coiled-coil domains were predicted using MacStripe 2.0b1 (Alex Knight 1998).

Antibodies

The anti-α-tubulin antibody DM1A was obtained from Sigma. The anti-PLK-1, anti-SPD-5, and anti-AIR-1 antibodies have been described (Chase et al., 2000; Hamill et al., 2002; Schumacher et al., 1998). Alexa Fluor 488 and 568 anti-mouse and anti-rabbit secondary antibodies were obtained from Molecular Probes.

Affinity-purified serum to SPD-2 was prepared using purified recombinant SPD-2 protein to immunize two rabbits at the Laboratory Animal Resources Facility of the University of Wisconsin Medical School. SPD-2-specific antibodies were then affinity purified using an immobilized MBP–SPD-2 fusion protein.

Immunocytochemistry and Microscopy

Indirect immunofluorescence was performed essentially as described (O'Connell et al., 2000). Primary antibodies were applied at a dilution of 1:500 to 1:5000, and secondary antibodies were applied at 1:200. For DNA staining, 0.3 μM TOT0-3 iodide (Molecular Probes) was included in the next-to-last wash. To disrupt microtubules, embryos were dissected from adult hermaphrodites in the presence of 50 μg/ml nocodazole, then allowed to incubate for 10 min at room temperature before fixation. Under these conditions, microtubules are completely depolymerized in about 1 min (Hamill et al., 2002).

Four-dimensional differential interference contrast imaging of *C. elegans* embryos was performed as described previously (O'Connell et al., 2000). Confocal imaging of live or fixed fluorescent specimens was performed on a Nikon Eclipse E800 scope equipped with a PerkinElmer Ultraview LCI CSU10 scanning unit, a Argon/Krypton ion laser (Melles Griot), and an ORCA ER cooled CCD camera (Hamamatsu). For live 4D imaging of GFP-expressing animals, embryos were mounted on agar pads and multiple focal planes 1–3 μm apart were acquired at specified time intervals. Image acquisition, analysis, and initial processing was done with PerkinElmer ImagingSuite software. To make fluorescence intensity measurements, we selected only those embryos in late prophase to avoid variability caused by developmental age. Measurements were made on projections of six focal planes that encompassed the entire MTOC by encircling the centrosome and subtracting background from an equal-sized region nearby. Additional image processing was done with Adobe Photoshop.

Acknowledgments

We are grateful to John White and Kevin Eliceiri for thoughtful advice and support, to Kara Maxwell and J. Michael Mullins for technical assistance, and to Bruce Bowerman, Danielle Hamill, Andy Golden, Pierre Gonczy, Sebastian Leidel, Yuji Kohara, Christian Malone, Jill Schumacher, Geraldine Seydoux, and Harold Smith for generously providing reagents and strains. P.Z. and J.A. were supported by the Wellcome Trust.

Received: October 2, 2003
Revised: February 6, 2004
Accepted: February 9, 2004
Published: April 12, 2004

References

Balczon, R. (1996). The centrosome in animal cells and its functional homologs in plant and yeast cells. Int. Rev. Cytol. *169*, 25–82.

Berdnik, D., and Knoblich, J.A. (2002). *Drosophila* Aurora-A is required for centrosome maturation and actin-dependent asymmetric protein localization during mitosis. Curr. Biol. *12*, 640–647.

Blagden, S.P., and Glover, D.M. (2003). Polar expeditions–provisioning the centrosome for mitosis. Nat. Cell Biol. *5*, 505–511.

Bobinnec, Y., Khodjakov, A., Mir, L.M., Rieder, C.L., Edde, B., and Bornens, M. (1998). Centriole disassembly in vivo and its effect on centrosome structure and function in vertebrate cells. J. Cell Biol. *143*, 1575–1589.

Bornens, M. (2002). Centrosome composition and microtubule anchoring mechanisms. Curr. Opin. Cell Biol. *14*, 25–34.

Bowerman, B. (2001). Cytokinesis in the *C. elegans* embryo: regulating contractile forces and a late role for the central spindle. Cell Struct. Funct. *26*, 603–607.

Brenner, S. (1974). The genetics of *Caenorhabditis elegans*. Genetics *77*, 71–94.

Chase, D., Serafinas, C., Ashcroft, N., Kosinski, M., Longo, D., Ferris, D.K., and Golden, A. (2000). The polo-like kinase PLK-1 is required for nuclear envelope breakdown and the completion of meiosis in *Caenorhabditis elegans*. Genesis *26*, 26–41.

Chen, Z., Indjeian, V.B., McManus, M., Wang, L., and Dynlacht, B.D. (2002). CP110, a cell cycle-dependent CDK substrate, regulates centrosome duplication in human cells. Dev. Cell *3*, 339–350.

Dai, W., Wang, Q., and Traganos, F. (2002). Polo-like kinases and centrosome regulation. Oncogene *21*, 6195–6200.

Dictenberg, J.B., Zimmerman, W., Sparks, C.A., Young, A., Vidair, C., Zheng, Y., Carrington, W., Fay, F.S., and Doxsey, S.J. (1998). Pericentrin and gamma-tubulin form a protein complex and are organized into a novel lattice at the centrosome. J. Cell Biol. *141*, 163–174.

do Carmo Avides, M., Tavares, A., and Glover, D.M. (2001). Polo kinase and Asp are needed to promote the mitotic organizing activity of centrosomes. Nat. Cell Biol. *3*, 421–424.

Donaldson, M.M., Tavares, A.A., Hagan, I.M., Nigg, E.A., and Glover, D.M. (2001a). The mitotic roles of Polo-like kinase. J. Cell Sci. *114*, 2357–2358.

Donaldson, M.M., Tavares, A.A., Ohkura, H., Deak, P., and Glover, D.M. (2001b). Metaphase arrest with centromere separation in *polo* mutants of *Drosophila*. J. Cell Biol. *153*, 663–676.

Doxsey, S.J., Stein, P., Evans, L., Calarco, P.D., and Kirschner, M. (1994). Pericentrin, a highly conserved centrosome protein involved in microtubule organization. Cell *76*, 639–650.

Fisk, H.A., and Winey, M. (2001). The mouse Mps1p-like kinase regulates centrosome duplication. Cell *106*, 95–104.

Gonczy, P. (2002). Mechanisms of spindle positioning: focus on flies and worms. Trends Cell Biol. *12*, 332–339.

Hamill, D.R., Severson, A.F., Carter, J.C., and Bowerman, B. (2002). Centrosome maturation and mitotic spindle assembly in *C. elegans* require SPD-5, a protein with multiple coiled-coil domains. Dev. Cell *3*, 673–684.

Hannak, E., Kirkham, M., Hyman, A.A., and Oegema, K. (2001). Aurora-A kinase is required for centrosome maturation in *Caenorhabditis elegans*. J. Cell Biol. *155*, 1109–1116.

Hannak, E., Oegema, K., Kirkham, M., Gonczy, P., Habermann, B., and Hyman, A.A. (2002). The kinetically dominant assembly pathway for centrosomal asters in *Caenorhabditis elegans* is gamma-tubulin dependent. J. Cell Biol. *157*, 591–602.

Hinchcliffe, E.H., Li, C., Thompson, E.A., Maller, J.L., and Sluder, G. (1999). Requirement of Cdk2-cyclin E activity for repeated centrosome reproduction in Xenopus egg extracts. Science *283*, 851–854.

Kamath, R.S., Martinez-Campos, M., Zipperlen, P., Fraser, A.G., and Ahringer, J. (2001). Effectiveness of specific RNA-mediated interference through ingested double-stranded RNA in *Caenorhabditis elegans*. Genome Biol *2*.

Katayama, H., Brinkley, W.R., and Sen, S. (2003). The Aurora kinases: role in cell transformation and tumorigenesis. Cancer Metastasis Rev. *22*, 451–464.

Kirkham, M., Muller-Reichert, T., Oegema, K., Grill, S., and Hyman, A.A. (2003). SAS-4 is a *C. elegans* centriolar protein that controls centrosome size. Cell *112*, 575–587.

Kuriyama, R., and Borisy, G.G. (1981). Centriole cycle in Chinese hamster ovary cells as determined by whole-mount electron microscopy. J. Cell Biol. *91*, 814–821.

Lacey, K.R., Jackson, P.K., and Stearns, T. (1999). Cyclin-dependent kinase control of centrosome duplication. Proc. Natl. Acad. Sci. USA *96*, 2817–2822.

Leidel, S., and Gonczy, P. (2003). SAS-4 is essential for centrosome

duplication in *C. elegans* and is recruited to daughter centrioles once per cell cycle. Dev. Cell *4*, 431–439.

Matthews, L.R., Carter, P., Thierry-Mieg, D., and Kemphues, K. (1998). ZYG-9, a *Caenorhabditis elegans* protein required for microtubule organization and function, is a component of meiotic and mitotic spindle poles. J. Cell Biol. *141*, 1159–1168.

Matsumoto, Y., Hayashi, K., and Nishida, E. (1999). Cyclin-dependent kinase 2 (Cdk2) is required for centrosome duplication in mammalian cells. Curr. Biol. *9*, 429–432.

Meraldi, P., Lukas, J., Fry, A.M., Bartek, J., and Nigg, E.A. (1999). Centrosome duplication in mammalian somatic cells requires E2F and Cdk2-cyclin A. Nat. Cell Biol. *1*, 88–93.

Moritz, M., Braunfeld, M.B., Guenebaut, V., Heuser, J., and Agard, D.A. (2000). Structure of the gamma-tubulin ring complex: a template for microtubule nucleation. Nat. Cell Biol. *2*, 365–370.

O'Connell, K.F. (2000). The centrosome of the early *C. elegans* embryo: inheritance, assembly, replication, and developmental roles. Curr. Top. Dev. Biol. *49*, 365–384.

O'Connell, K.F., Leys, C.M., and White, J.G. (1998). A genetic screen for temperature-sensitive cell-division mutants of *Caenorhabditis elegans*. Genetics *149*, 1303–1321.

O'Connell, K.F., Maxwell, K.N., and White, J.G. (2000). The *spd-2* gene is required for polarization of the anteroposterior axis and formation of the sperm asters in the *Caenorhabditis elegans* zygote. Dev. Biol. *222*, 55–70.

O'Connell, K.F., Caron, C., Kopish, K.R., Hurd, D.D., Kemphues, K.J., Li, Y., and White, J.G. (2001). The *C. elegans zyg-1* gene encodes a regulator of centrosome duplication with distinct maternal and paternal roles in the embryo. Cell *105*, 547–558.

Oegema, K., Wiese, C., Martin, O.C., Milligan, R.A., Iwamatsu, A., Mitchison, T.J., and Zheng, Y. (1999). Characterization of two related *Drosophila* gamma-tubulin complexes that differ in their ability to nucleate microtubules. J. Cell Biol. *144*, 721–733.

Okuda, M., Horn, H.F., Tarapore, P., Tokuyama, Y., Smulian, A.G., Chan, P.K., Knudsen, E.S., Hofmann, I.A., Snyder, J.D., Bove, K.E., and Fukasawa, K. (2000). Nucleophosmin/B23 is a target of CDK2/cyclin E in centrosome duplication. Cell *103*, 127–140.

Palazzo, R.E., Vogel, J.M., Schnackenberg, B.J., Hull, D.R., and Wu, X. (2000). Centrosome maturation. Curr. Top. Dev. Biol. *49*, 449–470.

Praitis, V., Casey, E., Collar, D., and Austin, J. (2001). Creation of low-copy integrated transgenic lines in *Caenorhabditis elegans*. Genetics *157*, 1217–1226.

Purohit, A., Tynan, S.H., Vallee, R., and Doxsey, S.J. (1999). Direct interaction of pericentrin with cytoplasmic dynein light intermediate chain contributes to mitotic spindle organization. J. Cell Biol. *147*, 481–492.

Ruiz, F., Beisson, J., Rossier, J., and Dupuis-Williams, P. (1999). Basal body duplication in *Paramecium* requires γ-tubulin. Curr. Biol. *9*, 43–46.

Salisbury, J.L., Suino, K.M., Busby, R., and Springett, M. (2002). Centrin-2 is required for centriole duplication in mammalian cells. Curr. Biol. *12*, 1287–1292.

Schnackenberg, B.J., Khodjakov, A., Rieder, C.L., and Palazzo, R.E. (1998). The disassembly and reassembly of functional centrosomes in vitro. Proc. Natl. Acad. Sci. USA *95*, 9295–9300.

Schumacher, J.M., Ashcroft, N., Donovan, P.J., and Golden, A. (1998). A highly conserved centrosomal kinase, AIR-1, is required for accurate cell cycle progression and segregation of developmental factors in *Caenorhabditis elegans* embryos. Development *125*, 4391–4402.

Shang, Y., Li, B., and Gorovsky, M.A. (2002). *Tetrahymena thermophila* contains a conventional gamma-tubulin that is differentially required for the maintenance of different microtubule-organizing centers. J. Cell Biol. *158*, 1195–1206.

Sluder, G., and Hinchcliffe, E.H. (1999). Control of centrosome reproduction: the right number at the right time. Biol. Cell. *91*, 413–427.

Stearns, T., and Kirschner, M. (1994). In vitro reconstitution of centrosome assembly and function: the central role of γ-tubulin. Cell *76*, 623–637.

Stein, L.D., Bao, Z., Blasiar, D., Blumenthal, T., Brent, M.R., Chen, N., Chinwalla, A., Clarke, L., Clee, C., Coghlan, A., et al. (2003). The genome sequence of *Caenorhabditis briggsae*: a platform for comparative genomics. PLoS Biol 1(2): e45 DOI:10.1371/journal.pbio.0000045.

Strome, S., Powers, J., Dunn, M., Reese, K., Malone, C.J., White, J., Seydoux, G., and Saxton, W. (2001). Spindle dynamics and the role of gamma-tubulin in early *Caenorhabditis elegans* embryos. Mol. Biol. Cell *12*, 1751–1764.

Tassin, A.M., and Bornens, M. (1999). Centrosome structure and microtubule nucleation in animal cells. Biol. Cell. *91*, 343–354.

Wiese, C., and Zheng, Y. (2000). A new function for the gamma-tubulin ring complex as a microtubule minus-end cap. Nat. Cell Biol. *2*, 358–364.

Zheng, Y., Wong, M.L., Alberts, B., and Mitchison, T. (1995). Nucleation of microtubule assembly by a γ-tubulin-containing ring complex. Nature *378*, 578–583.